

# **Numerical and analytical studies of current induced magnetization switching (CIMS) and back-hopping in MTJs with different thickness of MgO barrier**

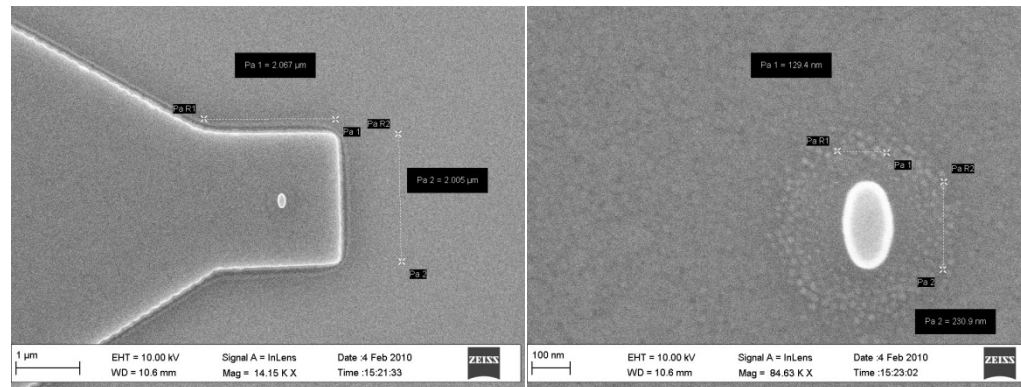
P. Ogrodnik(PW, IFM PAN), W. Skowroński(AGH),  
T. Stobiecki(AGH), J. Barnaś (IFM PAN)

**Transdisciplinary cooperation and applications of nanoscience**  
21-22 February 2013, Cracow,

## 1. Experimental data and background

- The following structure has been fabricated:

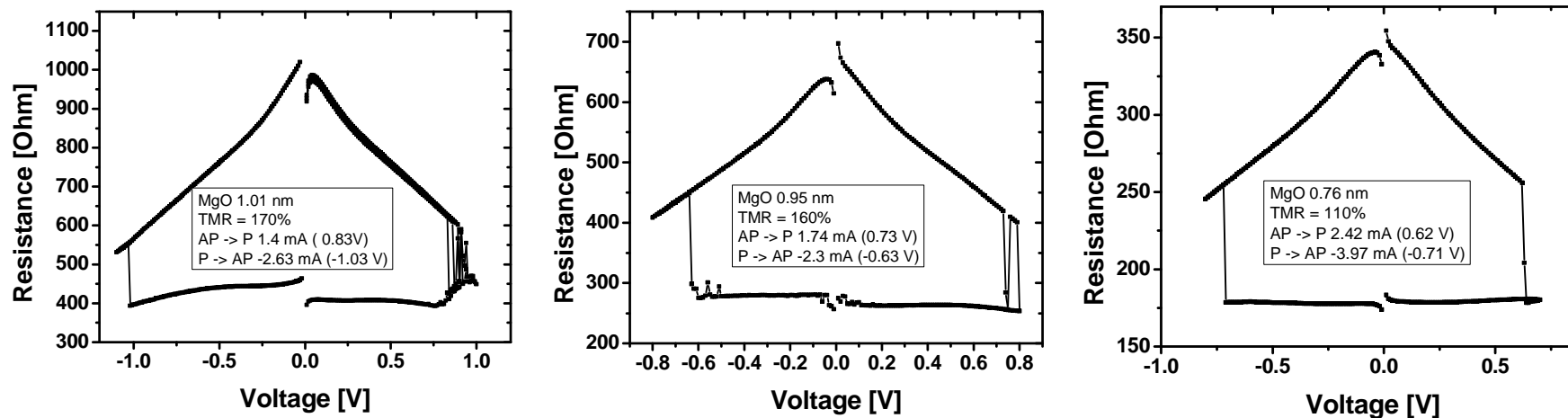
Ta(5) / CuN(50) / Ta(3) / CuN(50) / Ta(3) / PtMn (16) / Co<sub>70</sub>Fe<sub>30</sub>(2.1) / Ru(0.9) /  
Co<sub>40</sub>Fe<sub>40</sub>B<sub>20</sub>(2.3) / MgO(0.76 – 1.01) / Co<sub>40</sub>Fe<sub>40</sub>B<sub>20</sub>(2.3) / Ta(10) / CuN(30) / Ru(7)  
(thickness in nm)



Elliptical shape of nanopillars: 146 x 246 nm, area = 0.028  $\mu\text{m}^2$

Tunnel junctions with MgO barrier of thickness: 1.01 nm, 0.95 nm and 0.76 nm have been characterized.

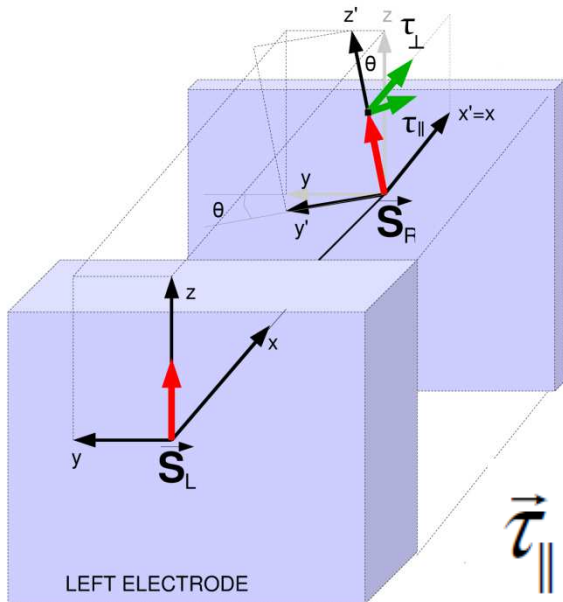
We focused on current induced switching in these 3 samples. Experimental resistance loops vs. bias are presented below:



For positive voltages (electrons flow from reference layer to the free one) we observe **back-hopping effect** (for MgO thickness 1.01 and 0.95 nm)

The aim is to simulate experimental resistance loops and description of dynamics in terms of linear stability analysis with use the switching phase diagram.

## 2. Model:



Dynamics described by  
Landau-Lifschitz-Gilbert equation:

$$\frac{d\vec{s}_R}{dt} + \alpha \vec{s}_R \times \frac{d\vec{s}_R}{dt} = \vec{\Gamma}$$

with current induced torques:

$$\vec{\tau}_{\parallel} = \tau_{\parallel} \vec{s}_R \times (\vec{s}_R \times \vec{s}_L) \quad \vec{\tau}_{\perp} = \tau_{\perp} \vec{s}_R \times \vec{s}_L$$

Dimensionless LLG equation in the spherical coordinates:

$$\left\{ \begin{array}{l} \frac{d\theta}{d\tau} = -\alpha \sin \theta \cos \theta - h_p \cos \phi \sin \theta \times \\ \times (\alpha \cos \theta \cos \phi + \sin \phi) - h_{\parallel} \sin \theta + \alpha h_{\perp} \sin \theta \\ \frac{d\phi}{d\tau} = -\cos \theta + h_p \cos \phi (\alpha \sin \phi - \cos \theta \cos \phi) + \\ + \alpha h_{\parallel} + h_{\perp} \end{array} \right. .$$

where:  $\tau$  - dimensionless time

$h_p = K_p / K$  - planar anisotropy

$h_{\perp} = \tau_{\perp} / 2Kd_f$   $h_{\parallel} = \tau_{\parallel} / 2Kd_f$  - normalized out-of-plane and in-plane torques

### 3. Method of linear stability analysis

We linearize the LLG equation near two main equilibrium points:  
 $\theta = 0$  (parallel state) and  $\theta = \pi$  (antiparallel state) for which:

$$\frac{d\theta}{d\tau} = 0, \frac{d\phi}{d\tau} = 0$$

Their stabilities (or unstabilities) can be determined from eigenvalues of linearized LLG equation.

For points corresponding to P and AP state, eigenvalues have the following forms:

$\theta = 0$ :

$$\mu_{1,2} = - \left\{ \frac{2h_{\parallel} + \alpha \left( (2 + h_p) - 2h_{\perp} \right)}{2} \pm \frac{\sqrt{-4\alpha^2 h_{\parallel}^2 + 4\alpha h_{\parallel} \left( (2 + h_p) - 2h_{\perp} \right) + \left( (-4 - 4h_p + \alpha^2 h_p^2) + 4(2 + h_p)h_{\perp} - 4h_{\perp}^2 \right)}}{2} \right\}$$

$\theta = \pi$ :

$$\mu_{1,2} = - \frac{1}{2} \left\{ 2\alpha - 2h_{\parallel} + \alpha h_p + 2\alpha h_{\perp} \pm \sqrt{-4 - 8\alpha h_{\parallel} - 4\alpha^2 h_{\parallel}^2 - 4h_p - 4\alpha h_{\parallel} h_p + \alpha^2 h_p^2 - 8h_{\perp} - 8\alpha h_{\parallel} h_{\perp} - 4h_p h_{\perp} - 4h_{\perp}^2} \right\}$$

Classifying the equilibrium points:

$$\mu_{1,2} = A \pm \sqrt{B}$$

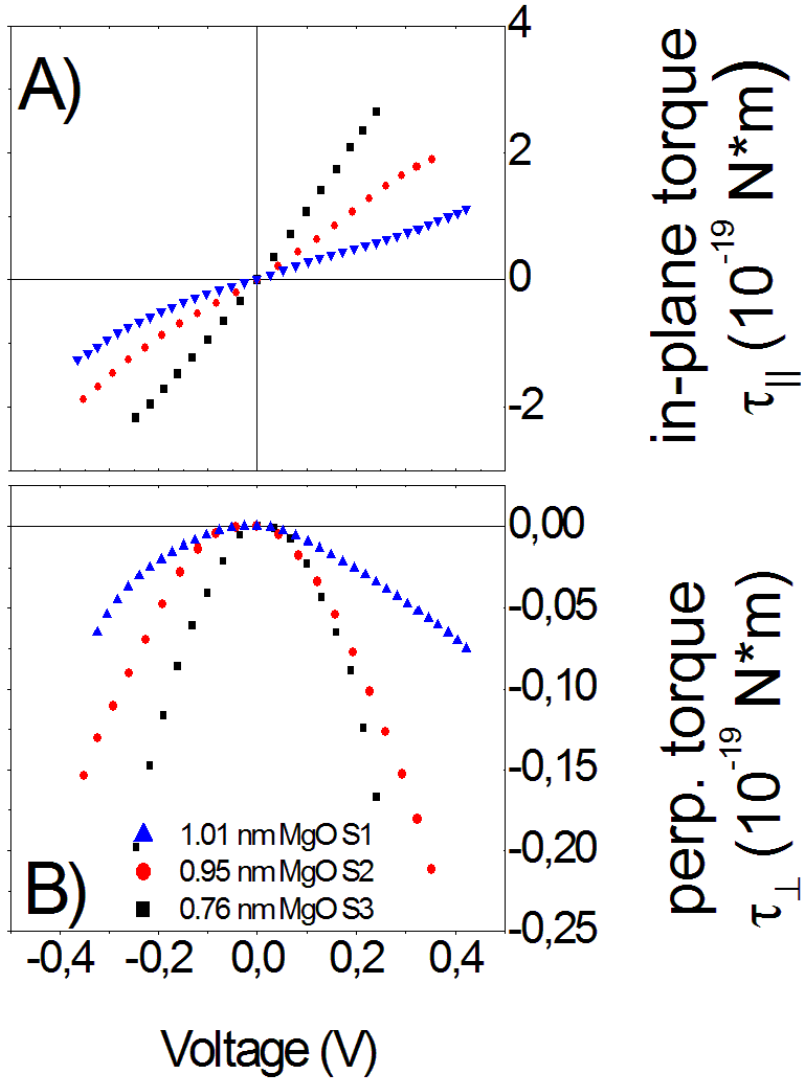
A	B	$\mu_{1,2}$	EQUILIBRIUM
-	-	Imaginary	Stable point
+	-	Imaginary	Unstable point
<b>Real</b>	+	$\mu_{1,2} < 0$	Stable point
<b>Real</b>	+	$\mu_{1,2} > 0$	Unstable point
<b>Real</b>	+	$\mu_1 < 0 < \mu_2$	Saddle point

Eigenvalues depend on  $h_p, h_{\perp, \parallel}, \alpha$ , which in our case can be measured.



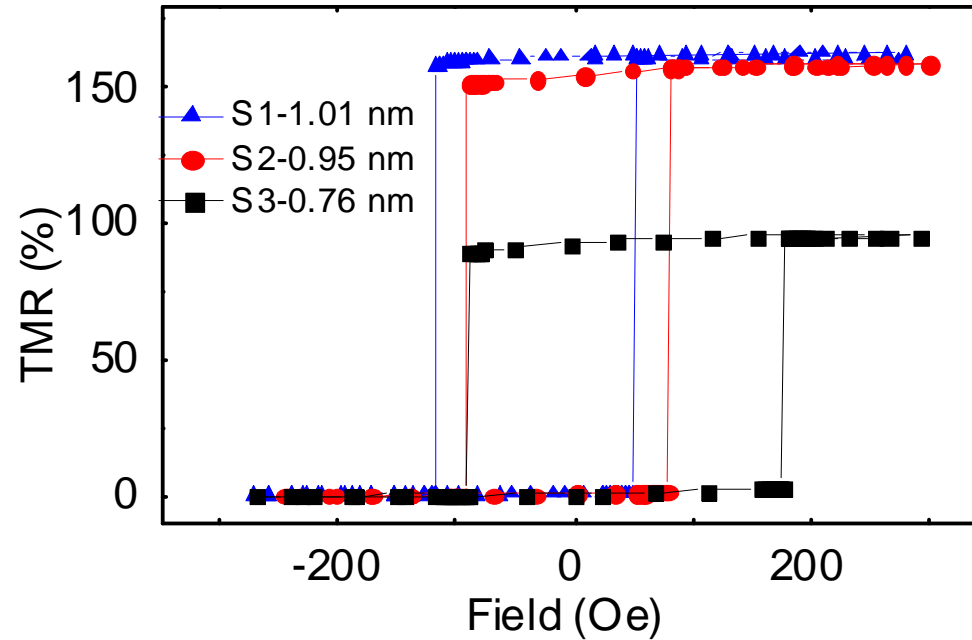
Dimensionless normal torque  $h_{\perp}$  consists of two parts: current induced torque and interlayer coupling. Interlayer coupling originates from exchange coupling of two magnetized layers as well as stray fields due to pillar shape of the structure.

All these components were measured in the experiment. The values of the other junctions' parameters and characteristics can be taken from experimental data as well:



Experimentally determined two components of current induced torques: in-plane component(top) and out-of-plane component(bottom).

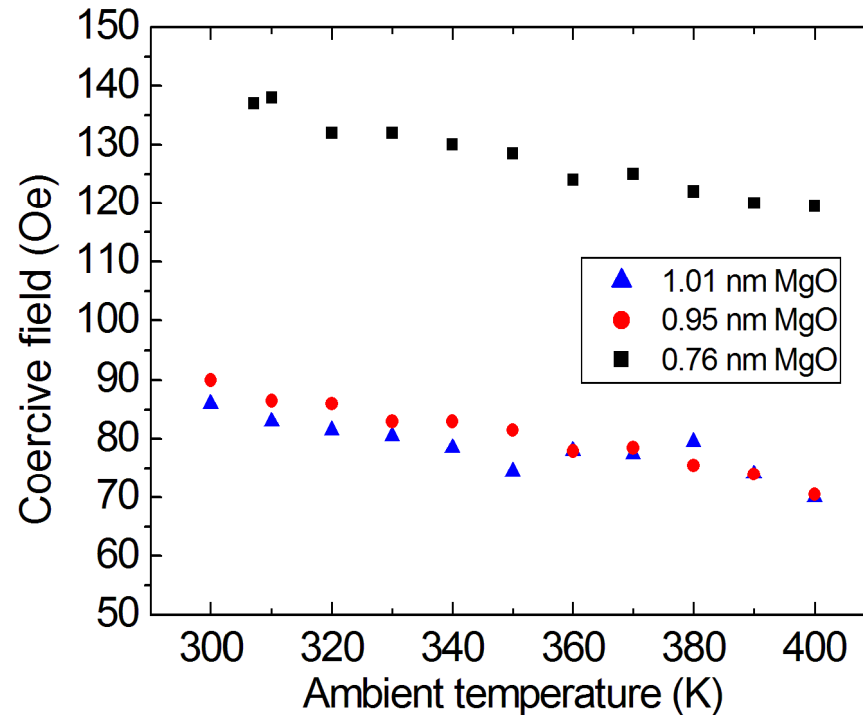
For  $|V| > 0.4$ , the experimental torques' determination is difficult due to low signal-to-noise ratio as well as the risk of junction's breakdown. Thus, in simulations, in-plane and out-of-plane torques' dependancies on higher voltages are extrapolated as linear and quadric functions respectively.



TMR loops for 3 samples with different MgO thickness

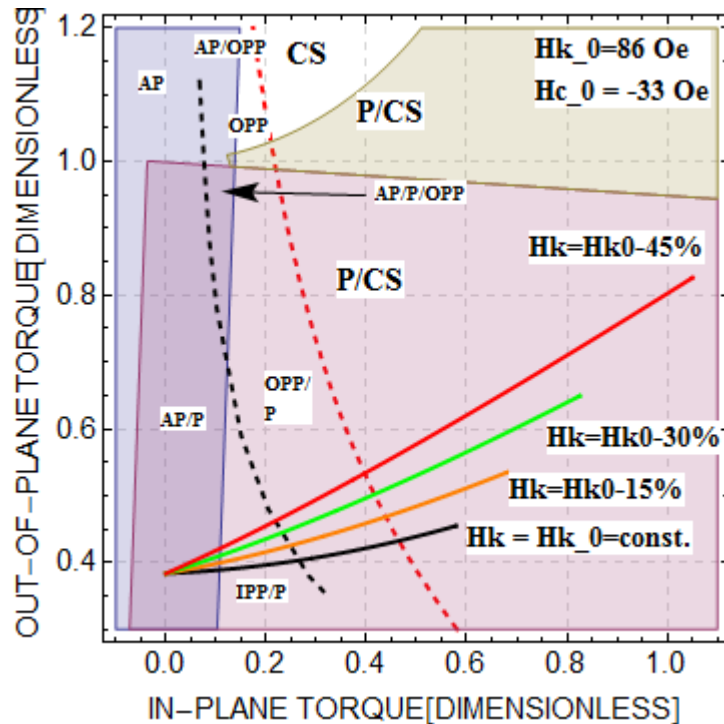
Sample	TMR	Total coupling field	Coercive field
S1(1.01 nm MgO)	165%	-33 Oe	86 Oe
S2(0.95 nm MgO)	160%	-10 Oe	90 Oe
S3(0.76 nm MgO)	100%	+44 Oe	134 Oe

Joule heating of junction influences on the coercive field. Simulations show that for bias of order 1V, the temperature of the junction rises to over 400K. It was necessary to find out how the increasing temperature decreases coercive field:





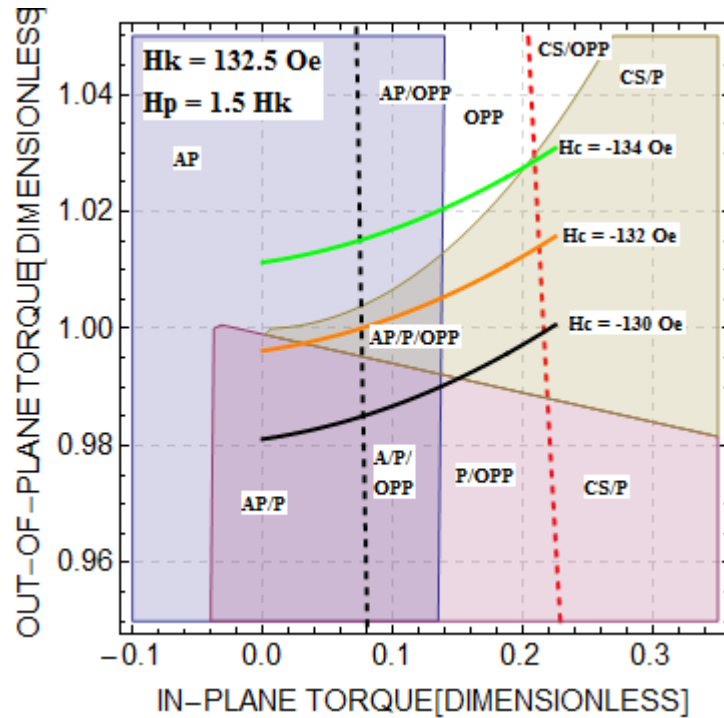
## The effect of coercive field reduction on the stability diagram



$Hk$  – coercive field,  
 $Hc_0$  – total coupling field

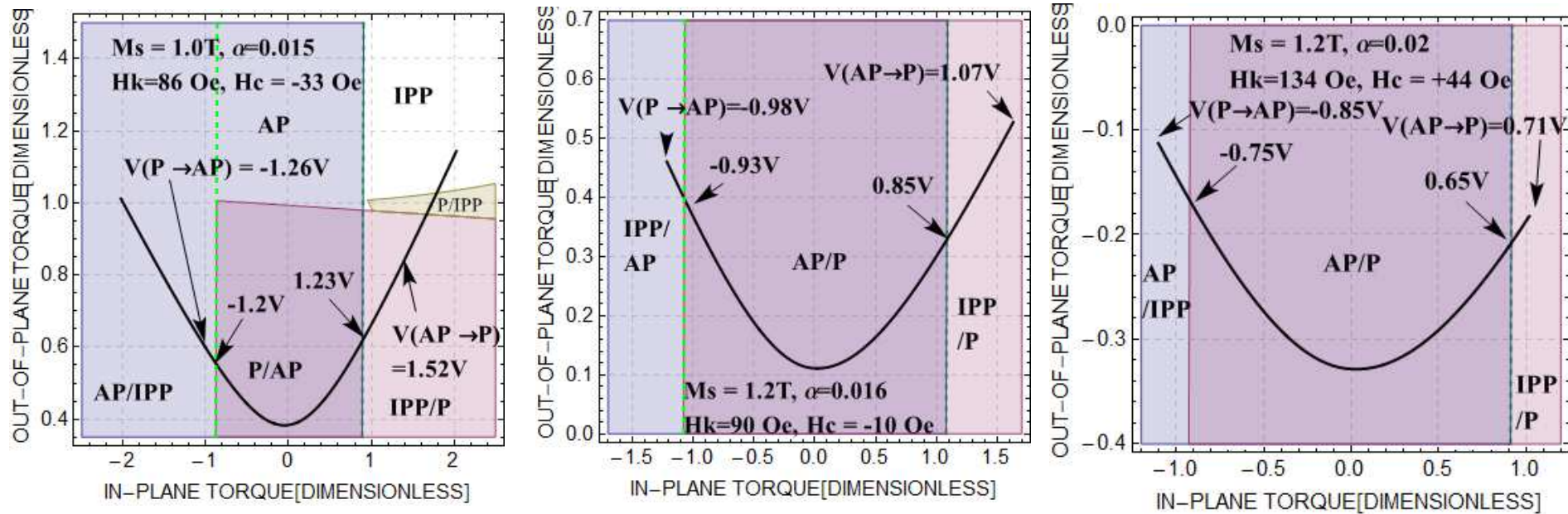
Color solid lines – experimental torques with different reduction of coercive field for voltages from 0V to 1V.

The effect of different interlayer coupling on stability diagram:



Change of  $H_c$  field (coupling Field) causes shift of torque lines (color solid lines) along the y-axis.

Experimental value of saturation magnetization allow to estimate anisotropy (according to formula  $E = \frac{1}{2} \mu_0 M_S^2$ ). We assume 30% reduction of coercive field for 1V. For the all parameters taken from the experiment we find the following diagrams:



S1 (1.01nm)

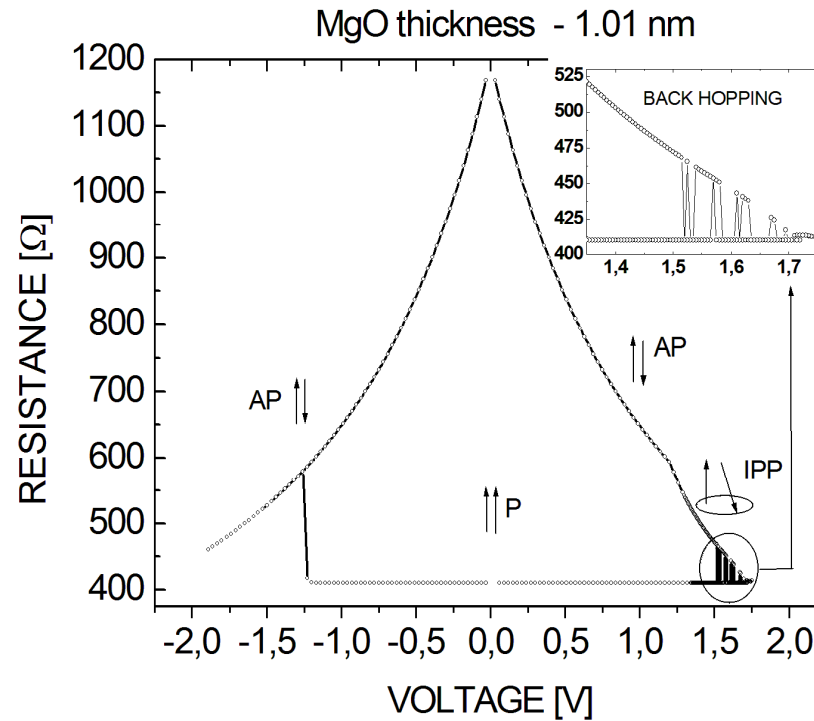
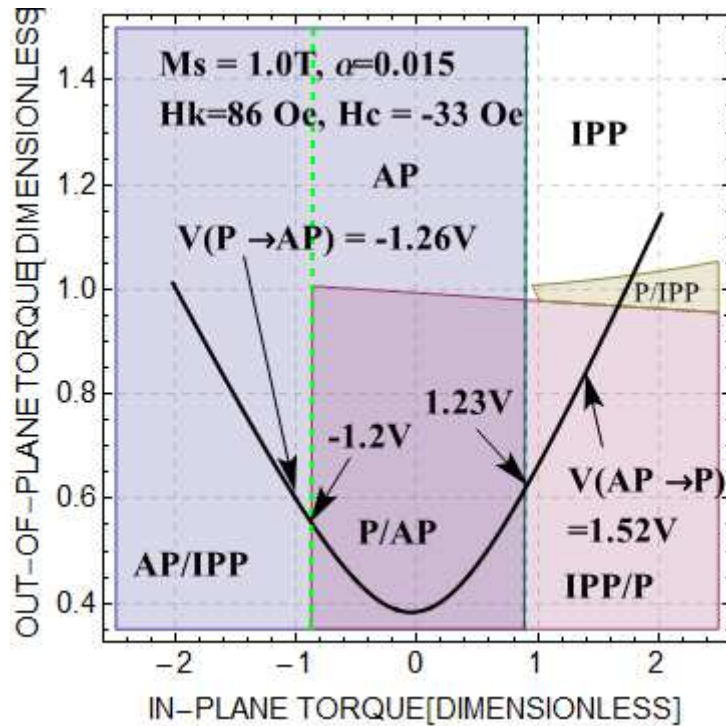
S2 (0.95nm)

S3(0.76nm)

IPP – inplane oscillations, black solid line – experimental torques

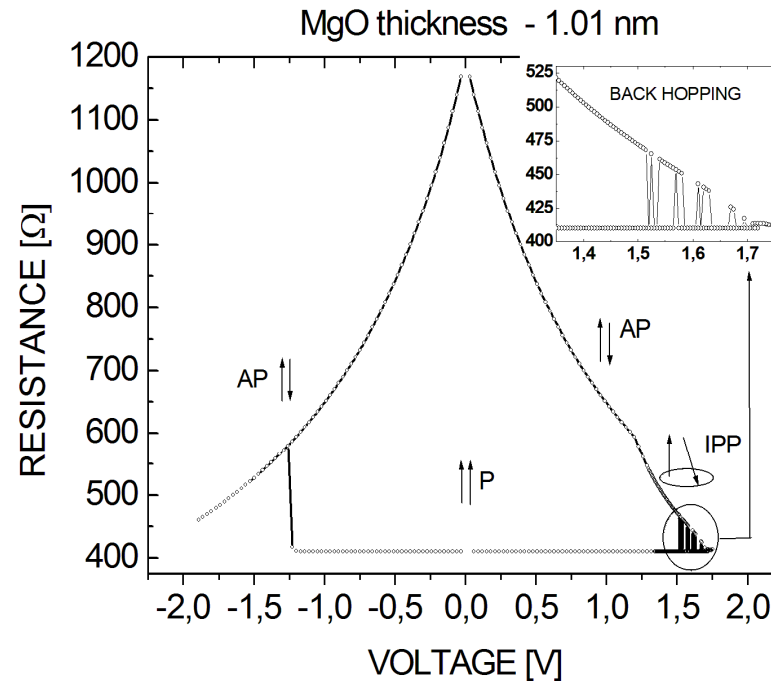
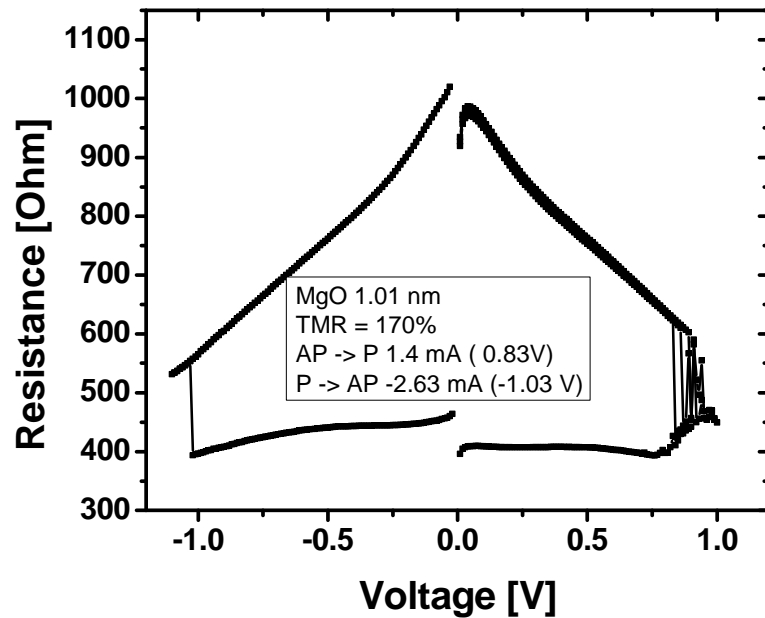


6. Numerical solution of the LLG equation versus switching diagram  
(S1 – 1.01 nm)



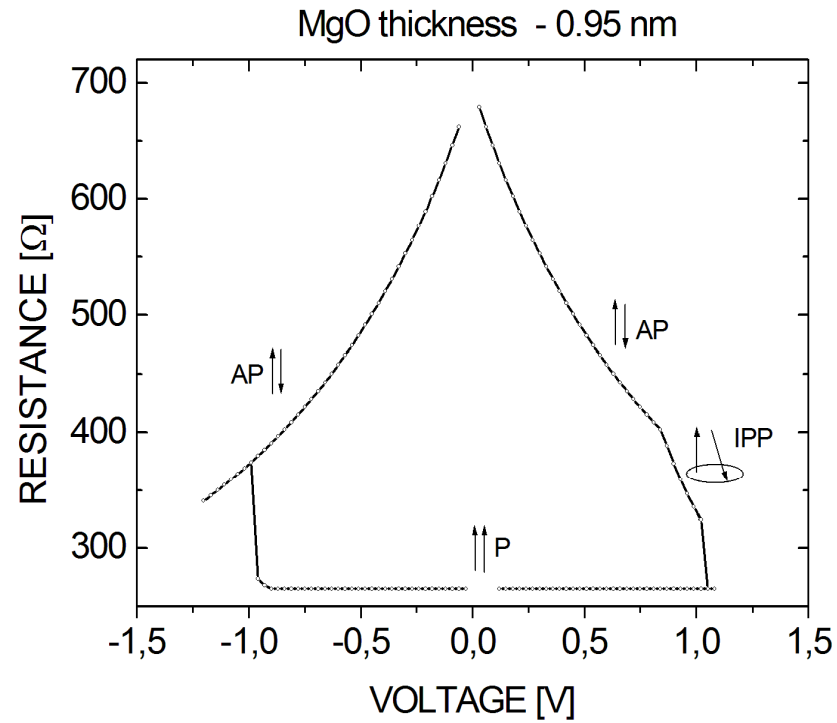
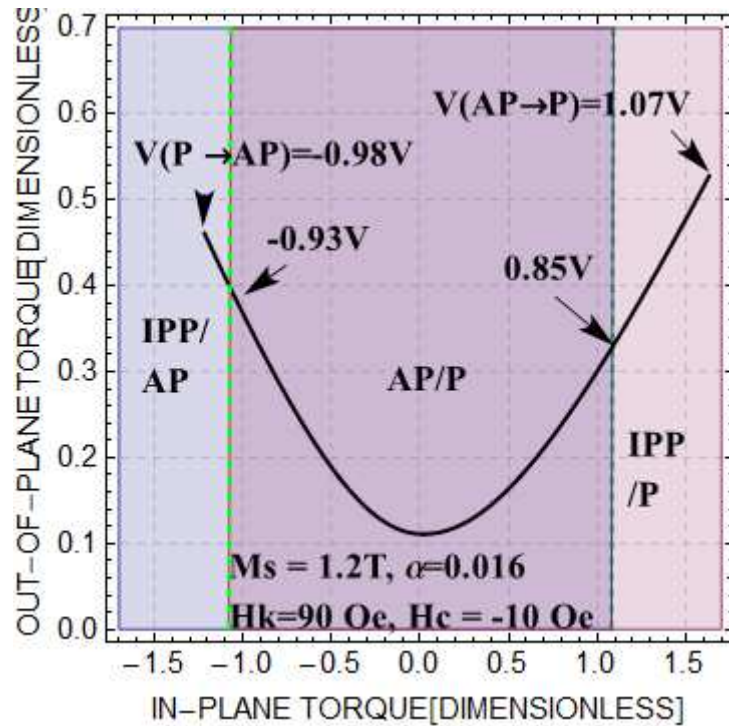
Back-hopping between IPP and P state occurs

Experiment vs. numerical simulation:



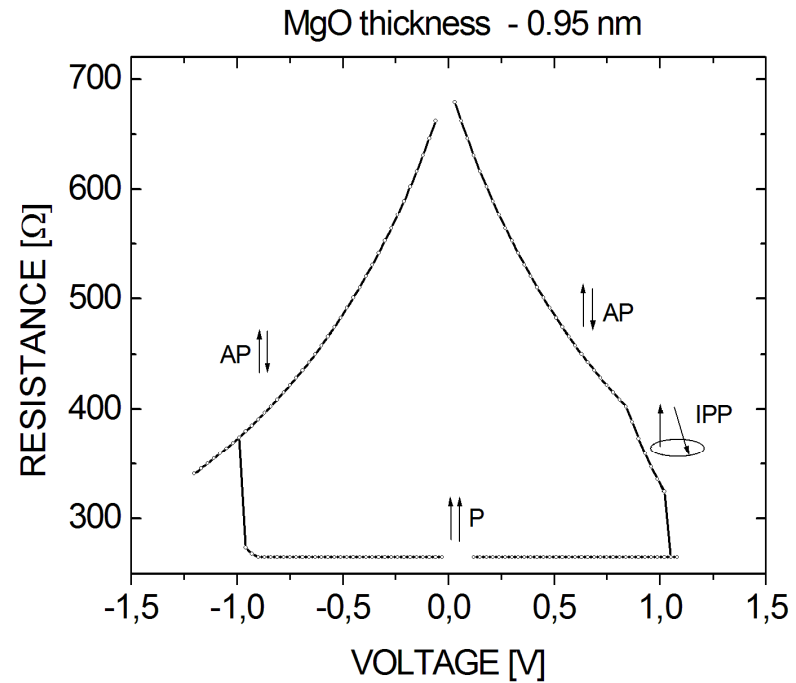
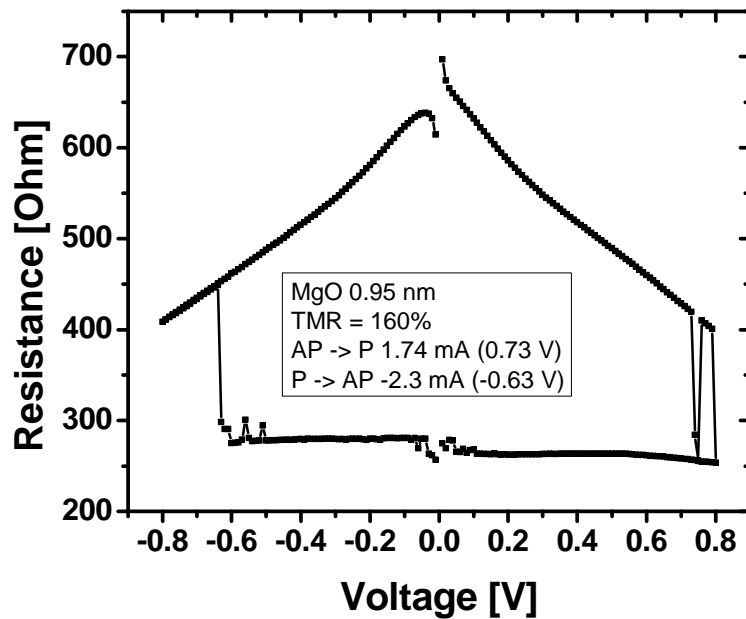
Back-hopping occurs at higher voltage but simulation qualitatively agrees with the experiment

7. Numerical solution of the LLG equation versus switching diagram  
(S2 – 0.95 nm)



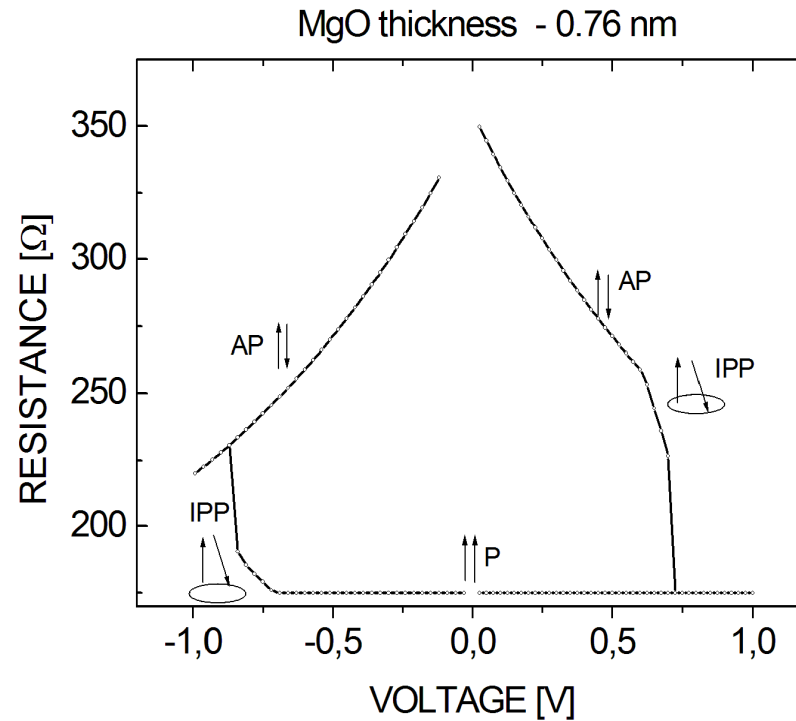
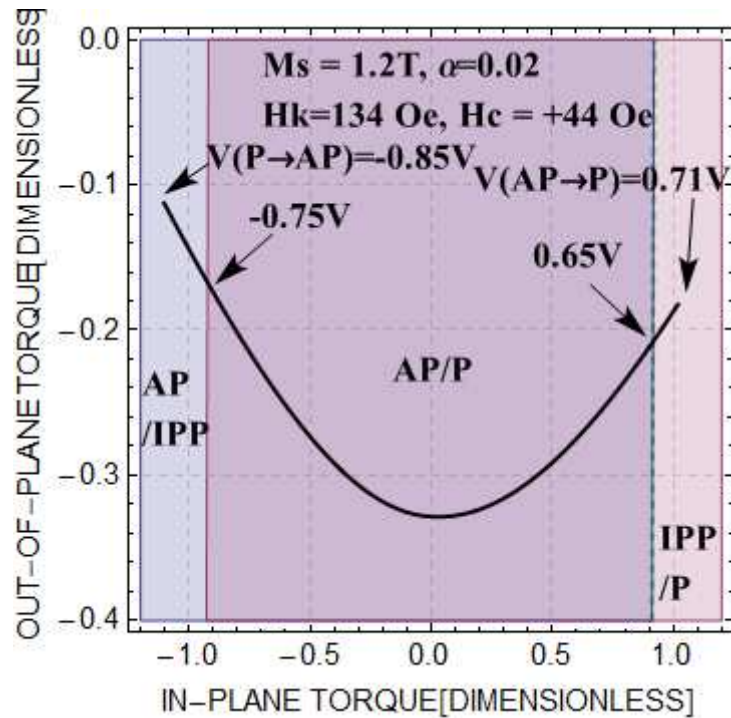
back-hopping – not observed (but still it is possible)

Experiment vs. numerical simulation:

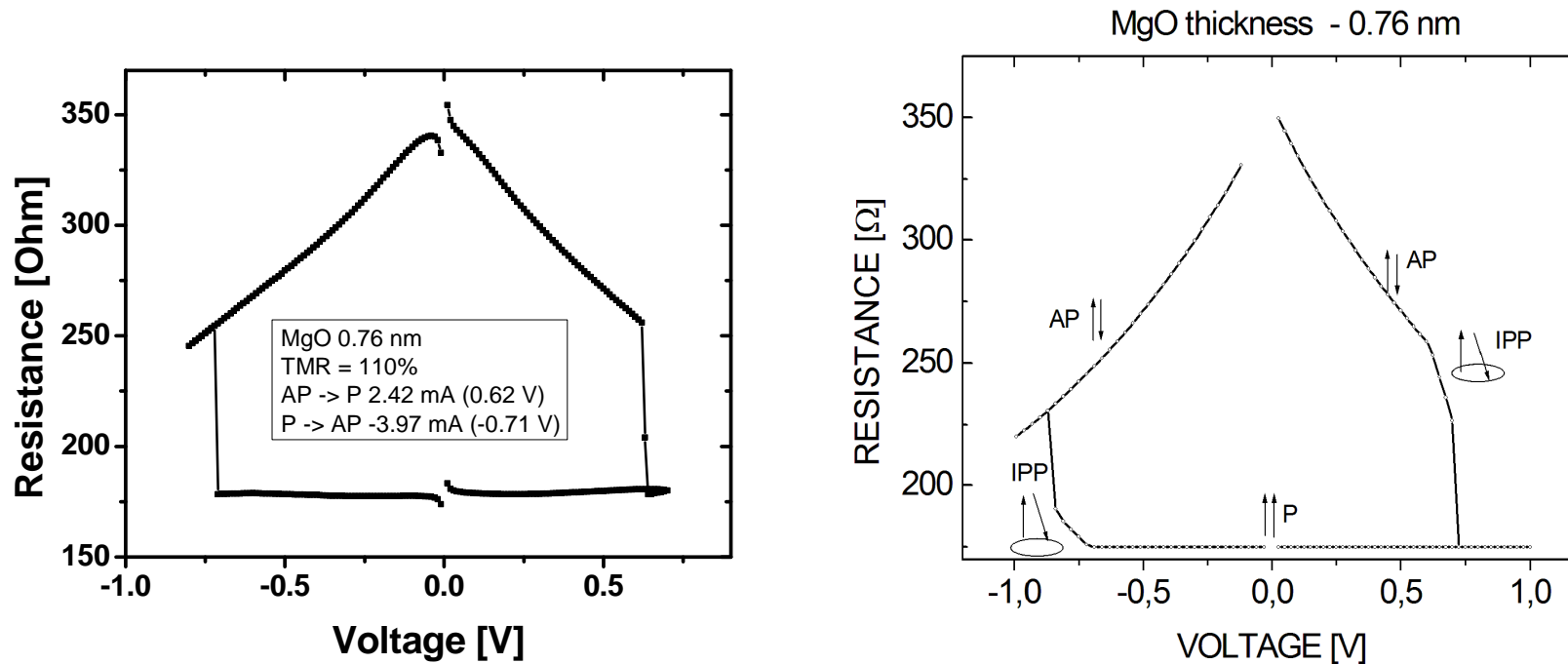


Back-hopping is limited to only one event. Probability of back-hopping is very low.

7. Numerical solution of the LLG equation versus switching diagram  
(S3 – 0.76 nm)



Experiment vs. numerical simulation:



Absence of back-hopping in the experiment as well as in the simulations. Switching occurs at similar voltages.

## Conclusions:

- We reproduced experimental resistance loops
- LLG equation allows to create the stability diagram which is consistent with experimental results.
- coupling influences on probability of back-hopping

Thank you for your attention



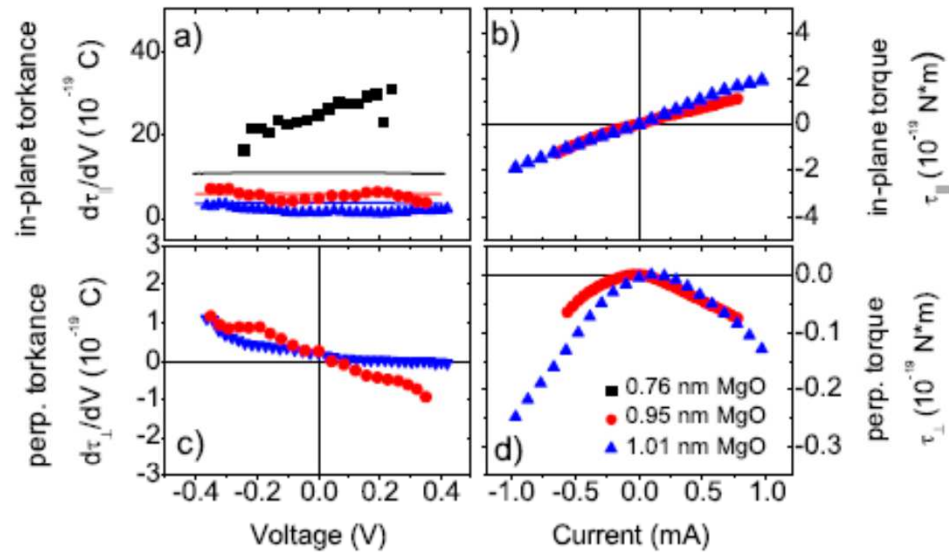


FIG. 5: Bias dependence of the in-plane torkance (a), in-plane torque (b), perpendicular torkance (c) and perpendicular torque (d) for MTJs with different MgO barrier thickness. The theoretical values in (a) (solid lines) were calculated using Eq. 3. Torque values are numerically integrated from measured torkances.

